Ultrasonic control of terahertz radiation via lattice anharmonicity in LiNbO3

R. H. Poolman, A. L. Ivanov, and E. A. Muljarov

Related Articles

Additional information on Appl. Phys. Lett.

Journal Homepage: http://apl.aip.org/

Journal Information: http://apl.aip.org/about/about_the_journal

Top downloads: http://apl.aip.org/features/most_downloaded

Information for Authors: http://apl.aip.org/authors

Ultrasonic control of terahertz radiation via lattice anharmonicity in LiNbO₃

R. H. Poolman,[a)] A. L. Ivanov, and E. A. Muljarov[b)]

School of Physics and Astronomy, Cardiff University, Cardiff CF24 3AA, United Kingdom

We propose a tunable terahertz (THz) filter using the resonant acousto-optic (RAO) effect. We present a design based on a transverse optical (TO) phonon mediated interaction between a coherent acoustic wave and the THz field in LiNbO₃. We predict a tunable range for the filter of up to 4 THz via the variation of the acoustic frequency between 0.1 and 1 GHz. The RAO effect in this case is due to cubic and quartic anharmonicities between TO phonons and the acoustic field. The effect of the interference between the anharmonicities is also discussed. © *2011 American Institute of Physics*. [doi:10.1063/1.3605569]

In recent years terahertz (THz) radiation has become a tool to study a wide variety of phenomena, necessitating the development of experimental techniques to access this spectral band.[1] Radiation in the THz range has been used to study picosecond phonon dynamics, polariton propagation, and optical properties of various materials and has been used for imaging purposes.[2–5] There are also several commercial applications that cover a variety of fields, including sub-mm wave astronomy, chemical recognition and biomedical imaging for disease diagnostics, and THz imaging and sensing for security applications.[6–8] As a result, spectrally resolved control of THz radiation has become an important research topic. One implementation uses optical control of carrier densities in type-I/type-II GaAs/AlAs multiple quantum wells at cryogenic temperatures.[9] Other implementations include magnetically tuned liquid crystals in metallic hole arrays and Lyot and Sloc filters, which were shown to be tunable over various ranges between 0.1 and 0.8 THz.[10–12] A relative lateral translation of two metallic photonic crystals has also resulted in a THz filter (tunable between 0.365 and 0.385 THz).[13]

In this letter, we show that the concept of the resonant acousto-optic (RAO) effect could be used to produce a tunable THz filter. We present a design and model numerically a LiNbO₃-based filter which is tunable in a wide range of up to 4 THz. The RAO effect which we use is, in general, a mediation of the interaction between an acoustic wave and a light field by a solid state excitation, when the light field and the excitation are in resonance.[14–18] In ionic crystals with soft TO-phonon modes, the interaction between a coherent acoustic wave and the THz field is mediated by a TO phonon.[17,18] The TO phonon is coupled to the acoustic wave via the anharmonicity present in the interatomic potential of the crystal lattice. This makes LiNbO₃ an excellent candidate for the filter, as it is both ionic and very strongly anharmonic. In fact, the strength of the anharmonicity in LiNbO₃ is such that both the cubic and quartic terms of the Taylor expansion of the interatomic potential have to be considered.

A schematic of the LiNbO₃-based tunable filter is shown in Fig. 1. A slab of LiNbO₃, less than 1 mm thick, is placed between narrow doped semiconductor contacts producing a resonator for ultrasound waves but at the same time transparent for THz light. Other options for the design include using the device as a reflection filter with only a lower doped layer. Owing to the phonon anharmonicities, two counter-propagating TO-phonon polariton waves in LiNbO₃, which are excited by an external THz light, can strongly couple to each other through the coherent acoustic field in the resonator. This happens at specific frequencies determined by the resonant Bragg condition.[18] At these resonant frequencies, acoustically induced transitions between TO-phonon states result in band gaps in the polariton dispersion creating peaks in the reflectivity. The anharmonic scattering channels responsible for these transitions are "TO phonon $\pm$ one (two) transverse acoustic phonon(s) $\rightarrow$ TO phonon," for the cubic (quartic) anharmonicity. The efficiency of these channels determines the width of the acoustically induced band gaps and the reflectivity spikes and increases with increasing acoustic intensity I_{ac}.[18]

To model numerically the RAO effect in the LiNbO₃ filter, we calculate reflectivity from the acoustically modulated semiconductor as well as extinction of the THz light inside a LiNbO₃ crystal. The acoustic wave parametrically modulates the semiconductor through the macroscopic polarization $\mathbf{P}(\mathbf{r},t)$ of TO phonons. This modulation can be expressed mathematically using the Hopfield model[19] of polaritons, generalized to the case of a parametric perturbation by an external coherent acoustic wave. The material equation for the TO-phonon polarization is then extended to the form[18]
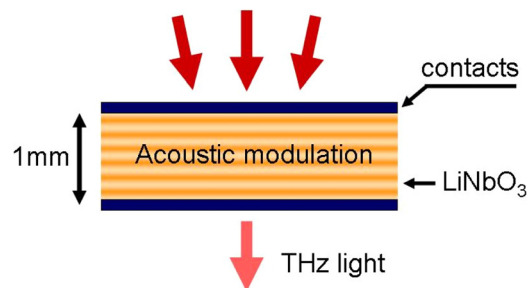
FIG. 1. (Color online) Schematic design of a LiNbO₃-based THz filter with an acoustic resonator.

a)Electronic mail: PoolmanRH@cardiff.ac.uk.
b)On leave from General Physics Institute RAS, Moscow, Russia. Electronic mail: egor.muljarov@astro.cf.ac.uk.

$$\frac{\varepsilon_b}{4\pi}\omega_R^2 \mathbf{E}(\mathbf{r},t) = \left[\frac{\partial^2}{\partial t^2} + 2\gamma_{TO}\frac{\partial}{\partial t} + \omega_{TO}^2\right]\mathbf{P}(\mathbf{r},t)$$
$$+ 2\omega_{TO}[m_3 I_{ac}^{1/2}(\mathbf{r},t)\cos(\Omega_{ac}t - \mathbf{Kr} + \phi_3)$$
$$+ 2m_4 I_{ac}(\mathbf{r},t)$$
$$+ m_4 I_{ac}(\mathbf{r},t)\cos(2\Omega_{ac}t - 2\mathbf{Kr} + 2\phi_4)]\mathbf{P}(\mathbf{r},t),$$

$$(1)$$

which includes both cubic and quartic terms of the coupling to the ultrasound wave, and in combination with Maxwell's equation and boundary conditions allows us to calculate the macroscopic electric field $\mathbf{E}(\mathbf{r},t)$. The standard material parameters ω_{TO}, γ_{TO}, and ω_R are the TO-phonon frequency, room temperature phenomenological TO-phonon damping, and the Rabi frequency of the Hopfield polariton, respectively. The background dielectric constant is given by ϵ_b. There are two controlling parameters for the RAO effect, the frequency of the acoustic wave $\Omega_{ac} = v_{ac}/(2\pi) = v_s K$, where $K = |\mathbf{K}|$ is the acoustic wave vector, and the strength of the coupling between the acoustic wave and the TO-phonon field. This coupling strength is controlled by the acoustic intensity $I_{ac}(\mathbf{r},t)$ and is given by $m_3 I_{ac}^{1/2}$ for cubic and $m_4 I_{ac}$ for quartic anharmonicity, the amplitudes of intrinsic coupling constants being $m_3 = 1.52 \times 10^7$ s$^{1/2}$g$^{-1/2}$ and $m_4 = 1.64$ s^{2}g^{-1} in LiNbO$_3$. The coupling constants are derived from the potential of the anharmonic components added to the Hopfield Hamiltonian.[17,20–22] In this paper, the coupling to a plane bulk acoustic wave with a moderate intensity $I_{ac}(\mathbf{r},t) = I_{ac} = 25$ kW/cm^2 is considered. The values of the phase shift $\phi = \phi_3 - \phi_4$ between the complex anharmonic coupling parameters in Eq. (1) are not available in the literature. Despite the large differences in coupling strength ($\hbar m_3 I_{ac}^{1/2} = 5.02$ meV, while $\hbar m_4 I_{ac} = 0.27$ meV) and the fact that the quartic modulation alone leads to negligibly small changes in the LiNbO$_3$ reflection, the cubic and quartic modulations interfere with each other resulting in noticeable ϕ-dependent effects which are also discussed below.

The modulation of the medium due to either cubic or quartic anharmonicities has been studied by us in Refs. 17,18. In this letter, we take into account both cubic and quartic modulations on an equal footing, including their interference. For collinear propagation of a THz light and an ultrasound wave, we calculate the Bragg scattering of the light by the acoustic wave, which is resonantly enhanced by the TO-phonon component of the polariton in LiNbO$_3$. To do so, we use the numerical method developed in Ref. 17. In particular, we solve numerically Eq. (1) in a semi-infinite LiNbO$_3$ region, using a superposition of partial polaritonic plane waves with all important Bragg harmonics taken into account. Because of the large strength of the mediated coupling we take into account up to 400 harmonics. Applying Maxwellian boundary conditions, we calculate the amplitudes of the partial waves of the transmitted and reflected electric field. Full details of the calculation method can be found in Ref. 18.

The total Bragg reflectivity, which includes all important Bragg replicas, calculated for the extreme cases of constructive ($\phi = 0$) and destructive interference ($\phi = \pi/2$) is compared in Fig. 2 with the TO-phonon polariton reflectivity
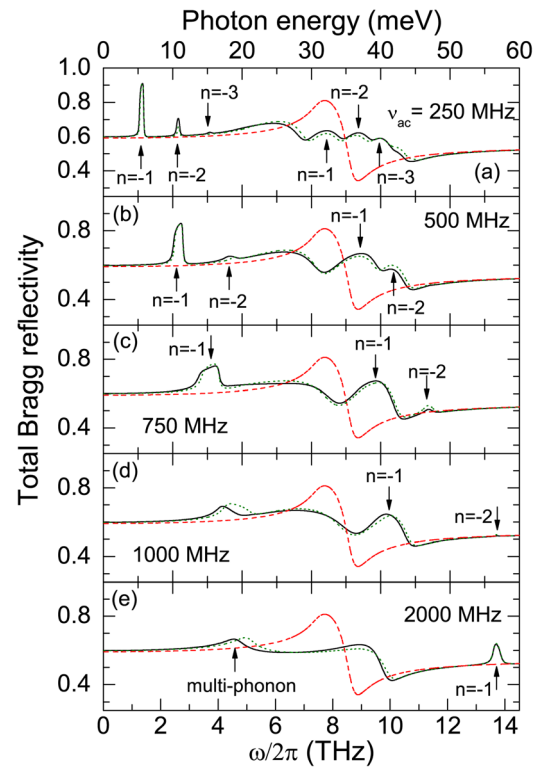
FIG. 2. (Color online) (a) to (e) show the development the THz reflection of LiNbO$_3$ with varying acoustic frequency and different phase shift between the cubic and quartic anharmonic parameters, $\phi = 0$ (black solid lines) and $\phi = \pi/2$ (green dotted lines). The dashed line is the reflectivity spectrum at $I_{ac} = 0$. In both cases, $\omega_{TO} = 31$ meV, $\omega_R = 18.0$ meV, $\gamma_{TO} = 1.26$ meV, and $\epsilon_b = 44$, see Ref. 21.

at $I_{ac} = 0$ (red dashed lines). The arrows indicate the peaks in the reflectivity caused by the gaps in the quasi-energy spectrum due to acoustically induced transitions between different TO-phonon polaritons. The peaks occur at the resonant Bragg condition $\omega = \omega_{pol}(nK/2)$ [$\omega_{pol}(k)$ is the TO-phonon polariton quasi-energy dispersion], both in the lower polariton (LP) and in the upper polariton (UP) branches, at the frequencies where co- and contra-propagating Bragg scattered polariton states are brought into resonance.[17,18]

The dramatic changes of the reflectivity peaks in a wide spectral range and, as suggested by the Bragg condition, their blue shift with increasing v_{ac} demonstrated in Fig. 2 are the phenomena which we propose to use for a widely tunable THz filter. The acoustic frequency provides an easy to manipulate parameter which allows for the tuning of the reflectivity. It can be clearly seen in Figs. 2(a)–2(d) that the light frequency range of $1 \leq \omega/(2\pi) \leq 4$ THz can be covered by the acoustic modulation of the LP branch with up to $v_{ac} \sim 1$ GHz.

The nth peak in the reflection physically corresponds to stimulated emission of $|n|$ dressed acoustic phonons and to down-conversion of the incoming THz light. In the LP branch, such dressing with higher-order processes of re-emission and re-absorption of acoustic phonons by the TO-phonon polariton becomes more and more efficient with increasing acoustic frequency v_{ac}, due to the flattening of the polariton dispersion near the bottom of the Restrahlen band and increasing of the TO-phonon fraction in the polariton states, which enhances their coupling to the acoustic wave. This results in widening of the lower peak with v_{ac} and even
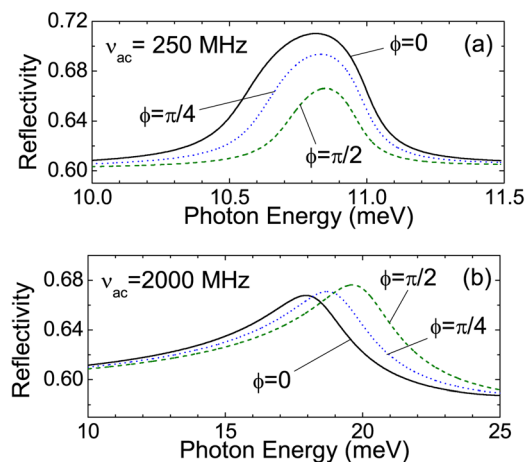
FIG. 3. (Color online) (a) The total Bragg reflectivity with the emphasis on the $n = -2$ Bragg signal in LP branch calculated for $\nu_{ac} = 250$ MHz and different phase: $\phi = 0$, $\pi/4$, and $\pi/2$. (b) The cumulative cups-like peak in the reflectivity spectrum calculated for $\nu_{ac} = 2$ GHz.

more pronounced spectral changes in the Restrahlen band itself, see Figs. 2(a)–2(e).

From Eq. (1), it is clear that the phase shift ϕ will only affect the peak, which is caused by both cubic and quartic anharmonicity. The cubic anharmonicity contributes to all Bragg signals ($n = -1$, $n = -2$, and so on), and the quartic anharmonicity contributes to even n only. This is why the strongest interference is observed for $n = -2$ Bragg signal which is detailed in Fig. 3(a) for different values of ϕ, see also Fig. 4(b). The peak position remains practically unaffected by ϕ as it is determined within this acoustic frequency range solely by the resonant Bragg condition. For high acoustic frequency, shown in Fig. 3(b), the line width and height of the LP peak are not greatly affected by the phase. However, the peak position is strongly ϕ-dependent because it is no longer determined by the Bragg condition. Instead, the individual acoustically induced band gaps accumulate at the bottom edge of the Restrahlen band to produce a cusp-like feature seen in Fig. 3(b), which is discussed in detail in Ref. 18.

To quantify the transmission through the LiNbO$_3$ slab we plot in Fig. 4 the extinction which is calculated as an inverse decay length of the electric field inside the slab. The spectra show a high contrast in THz light filtering as well as its wide-range tunability that demonstrates a large figure of merit of the proposed device.

In conclusion, our numerical modelling of the RAO effect in LiNbO$_3$ shows that there is potential for a THz filter that can be continuously tuned between 0.5 THz and ~ 4 THz. This could be achieved through the manipulation of the spectral position and height of peaks in reflectivity and extinction via the acousto-optical resonant Bragg condition.

FIG. 4. (Color online) Extinction of the electric field at different acoustic frequencies, for $\phi = 0$ (black solid lines) and $\phi = \pi/2$ (green dashed lines).

[1]C. A. Schmuttenmaer, Chem. Rev. **104**, 1759 (2004).
[2]J. C. Feurer, J. C. Vaughan, and K. A. Nelson, Science **299**, 374 (2003).
[3]S. Kojima, N. Tsumura, W. M. Takeda, and S. Nishizawa, Phys. Rev. B **67**, 035102 (2003).
[4]P. Y. Han and X.-C. Zhang, Meas. Sci. Technol. **12**, 1747 (2001).
[5]N. S. Stoyanov, D. W. Ward, T. Feurer, and K. A. Nelson, Nature Mat. **1**, 95 (2002).
[6]P. H. Siegel, IEEE Trans Microwave Theory Tech. **50**, 910 (2002).
[7]B. Fischer, M. Hoffmann, H. Helm, G. Modjesch, and P. U. Jepsen, Semicond. Sci. Technol. **20**, S246 (2005).
[8]J. F. Federici, B. Brian Schulkin, F. Huang, D. Gary, R. Barat, F. Oliveira, and D. Zimdars, Semicond. Sci. Technol. **20**, S266 (2005).
[9]I. H. Libon, S. Baumgärtner, M. Hemple, N. E. Hecker, J. Feldmann, M. Kock, and P. Dawson, Opt. Lett. **33**, 1401 (2008).
[10]C.-L. Pan, C.-F. Hsieh, R.-P. Pan, M. Tanaka, F. Miyamaru, M. Tani, and M. Hangyo, Opt. Express. **13**, 3921 (2005).
[11]C.-Y. Chen, C.-L. Pan, C.-F. Hsieh, Y.-F. Lin, and R.-P. Pan, Appl. Phys. Lett. **88**, 101107 (2006).
[12]I.-C. Ho, C.-L. Pan, C.-F. Hsieh, and R.-P. Pan, Opt. Lett. **33**, 1401 (2008).
[13]T. D. Drysdale, I. S. Gregory, C. Baker, E. H. Linfield, W. R. Tribe, and D. R. S. Cumming, Appl. Phys. Lett. **85**, 5173 (2004).
[14]A. L. Ivanov and P. Littlewood, Phys. Rev. Lett. **87**, 136403 (2001).
[15]A. L. Ivanov, Phys. Status. Solidi A **202**, 2657 (2005).
[16]A. L. Ivanov, in *Problems of Condensed Matter Physics*, edited by A. L. Ivanov and S. G. Tikhodeev (Oxford University, Oxford, 2008) pp. 301–322.
[17]R. H. Poolman, E. A. Muljarov, and A. L. Ivanov, Phys. Rev. B **81**, 245208 (2010).
[18]E. A. Muljarov, R. H. Poolman, and A. L. Ivanov, Phys. Rev. B **83**, 115204 (2011).
[19]J. J. Hopfield and D. G. Thomas, Phys. Rev. **132**, 563 (1963).
[20]V. Romero-Rochín, R. M. Kochl, C. J. Brennan, and K. A. Nelson, J. Chem. Phys. **111**, 3559 (1999).
[21]S. C. Abrahams, in *Properties of Lithium Niobate*, edited by K. K. Wong (The Institute of Electrical Engineers, London, United Kingdom 2002).
[22]J. Menéndez and M. Cardona, Phys. Rev. B **29**, 2051 (1984).